

Sodium Iodide Symporter (NIS)-Mediated Radionuclide (^{131}I , ^{188}Re) Therapy of Liver Cancer After Transcriptionally Targeted Intratumoral *in Vivo* NIS Gene Delivery

Kathrin Klutz,¹ Michael J. Willhauck,¹ Nathalie Wunderlich,¹ Christian Zach,² Martina Anton,³ Reingard Senekowitsch-Schmidtke,⁴ Burkhard Göke,¹ and Christine Spitzweg¹

Abstract

We reported the therapeutic efficacy of ^{131}I in hepatocellular carcinoma (HCC) cells stably expressing the sodium iodide symporter (NIS) under the control of the tumor-specific α -fetoprotein (AFP) promoter. In the current study we investigated the efficacy of adenovirus-mediated *in vivo* NIS gene transfer followed by ^{131}I and ^{188}Re administration for the treatment of HCC xenografts. We used a replication-deficient adenovirus carrying the human NIS gene linked to the mouse AFP promoter (Ad5-AFP-NIS) for *in vitro* and *in vivo* NIS gene transfer. Functional NIS expression was confirmed by *in vivo* γ -camera imaging, followed by analysis of NIS protein and mRNA expression. Human HCC (HepG2) cells infected with Ad5-AFP-NIS concentrated 50% of the applied activity of ^{125}I , which was sufficiently high for a therapeutic effect in an *in vitro* clonogenic assay. Four days after intratumoral injection of Ad5-AFP-NIS (3×10^9 plaque-forming units) HepG2 xenografts accumulated 14.5% injected dose (ID)/g ^{123}I with an effective half-life of 13 hr (tumor-absorbed dose, 318 mGy/MBq ^{131}I). In comparison, 9.2% ID/g ^{188}Re was accumulated in tumors with an effective half-life of 12.8 hr (tumor-absorbed dose, 545 mGy/MBq). After adenovirus-mediated NIS gene transfer in HepG2 xenografts administration of a therapeutic dose of ^{131}I or ^{188}Re (55.5 MBq) resulted in a significant delay in tumor growth and improved survival without a significant difference between ^{188}Re and ^{131}I . In conclusion, a therapeutic effect of ^{131}I and ^{188}Re was demonstrated in HepG2 xenografts after tumor-specific adenovirus-mediated *in vivo* NIS gene transfer.

Introduction

HEPATOCELLULAR CARCINOMA (HCC) is a common cancer with increasing incidence worldwide. Despite novel treatment strategies including cryosurgery, radiofrequency thermal ablation, and chemoembolization, the prognosis of patients with advanced HCC has remained poor. Therefore, the development of alternative therapeutic approaches is urgently needed.

The sodium iodide symporter (NIS) mediates the active transport of iodide across the basolateral membrane of thyroid cells and represents the molecular basis for the diagnostic and therapeutic application of radioiodine, which has been successfully used for more than 70 years in the treatment of patients with thyroid cancer (Spitzweg *et al.*, 2001b;

Hingorani *et al.*, 2010). Since its cloning in 1996 NIS has been characterized as a novel promising target gene for the development of a novel gene therapy strategy based on selective NIS gene transfer into tumor cells followed by diagnostic and therapeutic application of radioiodine (Dai *et al.*, 1996; Smanik *et al.*, 1996; Spitzweg *et al.*, 1999, 2000, 2001a,b, 2007; Spitzweg and Morris, 2002; Kakinuma *et al.*, 2003; Dingli *et al.*, 2004; Cengic *et al.*, 2005; Dwyer *et al.*, 2005a; Scholz *et al.*, 2005; Willhauck *et al.*, 2007, 2008a,b; Trujillo *et al.*, 2010; Hingorani *et al.*, 2010; Li *et al.*, 2010; Penheiter *et al.*, 2010). To achieve tumor selectivity, functional NIS gene expression can be transcriptionally targeted by application of tissue- or tumor-specific promoters (Hart, 1996; Peerlinck *et al.*, 2009). In an earlier study in a liver cancer mouse model, we applied a mouse α -fetoprotein (AFP) promoter construct consisting of

¹Department of Internal Medicine II, Ludwig Maximilians University, Munich 81377, Germany.

²Department of Nuclear Medicine, Ludwig Maximilians University, Munich 81377, Germany.

³Institute of Experimental Oncology, Technical University Munich, Munich 81675, Germany.

⁴Department of Nuclear Medicine, Technical University Munich, Munich 81675, Germany.

the basal promoter and enhancer I to drive NIS expression and demonstrated tumor-specific iodide accumulation in stably transfected hepatocellular carcinoma cells, which showed a significant inhibition of growth when xenografted in nude mice after application of ^{131}I (Willhauck *et al.*, 2008b).

To further improve the NIS gene therapy concept toward a possible clinical application, in the current study we developed a replication-deficient adenovirus carrying the human NIS gene linked to the same AFP promoter construct (Ad5-AFP-NIS) that allows *in vivo* NIS gene delivery.

Because extrathyroidal tumors are not able to organify iodide after NIS gene transfer, the limited iodide retention time may hamper the therapeutic efficacy of ^{131}I therapy. The application of rhenium-188, which is also transported via NIS, but characterized by a shorter physical half-life and decay properties superior to ^{131}I , may provide a powerful tool to enhance the therapeutic efficacy of NIS-mediated radionuclide therapy, in particular because of its enhanced crossfire effect (maximal path length of up to 10.4 mm). ^{188}Re has already been successfully used by our own group to enhance the therapeutic efficacy of NIS-mediated radionuclide therapy in a prostate cancer xenograft model (Willhauck *et al.*, 2007). In addition, Dadachova and colleagues demonstrated a more pronounced growth-inhibiting effect in NIS-expressing mammary tumors in a transgenic mouse model after application of ^{188}Re (Dadachova *et al.*, 2005).

In the current study, we therefore examined the accumulation and therapeutic efficacy of ^{131}I in direct comparison with ^{188}Re in an HCC xenograft mouse model after tumor-specific, adenovirus-mediated *in vivo* NIS gene transfer.

Materials and Methods

Cell culture

The human HCC cell line HepG2 (HB-8065; American Type Culture Collection [ATCC], Manassas, VA) and the human prostate cancer cell line LNCaP (CRL-1740; ATCC) were cultured in RPMI (Invitrogen Life Technologies, Karlsruhe, Germany) supplemented with fetal bovine serum (10%, v/v; PAA, Cölbe, Germany) and penicillin–streptomycin (1%, v/v). The human melanoma cell line 1205Lu (kindly provided by M. Herlyn, Wistar Institute, Philadelphia, PA) was grown in MCDB 153 medium (Invitrogen Life Technologies) supplemented with Leibovitz's L-15 medium (20%, v/v; Invitrogen Life Technologies), fetal bovine serum (2%, v/v), insulin (5 $\mu\text{g}/\text{ml}$; Sigma, Munich Germany), and penicillin–streptomycin (1%, v/v). Cells were maintained at 37°C and 5% CO_2 in an incubator with 95% humidity. The cell culture medium was replaced every second day and cells were passaged at 85% confluency.

Recombinant adenovirus production

A replication-deficient human recombinant type 5 adenovirus (Ad5) carrying the human NIS gene linked to a mouse AFP promoter construct consisting of the basal promoter and enhancer element I (Willhauck *et al.*, 2008b) (kindly provided by M. Geissler, Esslingen, Germany) was developed in collaboration with ViraQuest (North Liberty, IA) (Ad5-AFP-NIS). The human NIS cDNA was cut from the pcDNA plasmid (kindly provided by S.M. Jhiang, Ohio State University, Columbus, OH), using *EcoRI*, and cloned into the

shuttle vector pVQAd-AscI-NpA. The AFP promoter construct was cloned into pVQAd-AscI-NpA, using *KpnI* and *XhoI*. The resulting shuttle vector construct contains the full-length NIS cDNA coupled to the AFP promoter.

As controls, a replication-deficient adenovirus carrying the NIS cDNA under the control of the unspecific cytomegalovirus (CMV) promoter generated as described previously (Ad5-CMV-NIS) (Spitzweg *et al.*, 2001a) and an empty virus (Ad5-control) were used.

Adenovirus-mediated NIS gene transfer in vitro

For *in vitro* infection experiments, HepG2 or control cells (LNCaP and 1205Lu) (1.5×10^5 cells/ml in 12-well plates) were washed and incubated for 2.5 hr with Opti-MEM (Invitrogen Life Technologies) containing Ad5-AFP-NIS (multiplicity of infection [MOI], 60). Medium was replaced by fresh culture medium and virus-infected cells were further maintained for 4 days, before iodide accumulation was measured (see below) to determine levels of functional NIS protein expression. All adenoviral infections were carried out at least in triplicates.

^{125}I uptake assay

After infection with Ad5-AFP-NIS or Ad5-control, iodide uptake of HepG2 or control cells was determined under steady state conditions (Weiss *et al.*, 1984) as described previously (Spitzweg *et al.*, 1999). KClO_4 as a competitive inhibitor of NIS was added to control wells. Results were normalized to cell viability and expressed as counts per minute relative to number of living cells, as represented by absorbance at 490 nm ($\text{cpm}/A_{490\text{nm}}$).

Cell viability assay

Cell viability was measured with a commercially available MTS [3-(4,5-dimethylthiazol-2-yl)-5-(3-carboxymethoxyphenyl)-2-(4-sulfophenyl)-2H-tetrazolium] assay (Promega, Mannheim, Germany) according to the manufacturer's recommendations as described previously (Unterholzner *et al.*, 2006).

Clonogenic assay

HepG2 cells were infected with Ad5-AFP-NIS (60 MOI) as described previously. Four days after infection, cells were incubated for 7 hr with 29.6 MBq (0.8 mCi), 14.8 MBq (0.4 mCi), or 7.4 MBq (0.2 mCi) of ^{131}I or saline in Hanks' balanced salt solution supplemented with 10 μM NaI and 10 mM HEPES (pH 7.3) at 37°C. As a further control noninfected cells were incubated with 29.6 MBq of ^{131}I . After incubation with ^{131}I or saline, a clonogenic assay was performed as described previously (Mandell *et al.*, 1999; Spitzweg *et al.*, 2000).

Establishment of xenograft tumors in nude mice

HepG2 and 1205Lu xenografts were established in 5-week-old female CD-1 *nu/nu* mice (Charles River, Sulzfeld, Germany) by subcutaneous injection, into the flank region, of 1×10^7 HepG2 cells suspended in 100 μl of phosphate-buffered saline (PBS) and 100 μl of Matrigel basement membrane matrix (BD Biosciences, San Jose, CA) or 1.5×10^6 1205Lu cells suspended in 100 μl of PBS. LNCaP xenografts

were established in male CD-1 *nu/nu* mice by subcutaneous injection, into the flank region, of 1×10^6 cells suspended in 250 μ l of PBS and 250 μ l of Matrigel basement membrane matrix (BD Biosciences). Animals were maintained under specific pathogen-free conditions with access to mouse chow and water *ad libitum*. The experimental protocol was approved by the regional governmental commission for animals (Regierung von Oberbayern, Munich, Germany).

Adenovirus-mediated NIS gene delivery in xenograft tumors in nude mice

Experiments started when tumors had reached a size of 3–5 mm. After a 10-day pretreatment with L-thyroxine (L-T4; Sanofi-Aventis, Frankfurt am Main, Germany) (5 mg/liter) in their drinking water to maximize radioiodine uptake in tumor and to reduce iodide uptake by the thyroid gland, animals were anesthetized with ketamine (100 μ g/g; Hameln Pharmaceuticals, Hameln, Germany) and xylazine (2%, v/v; Bayer, Leverkusen, Germany) (10 μ g/g). Thereafter, 3×10^9 plaque-forming units (PFU) (diluted with PBS to a total volume of 100 μ l) of the recombinant Ad5-AFP-NIS or Ad5-control was injected at five different injection sites directly into the tumor, using tuberculin syringes with a 30-gauge \times 0.5-inch needle. The needle was moved to various sites within the tumor during injection to maximize the area of virus exposure. To investigate tumor specificity of the virus construct in the case of virus leakage, a cohort of tumor-bearing mice received 3×10^9 PFU of either the nonspecific Ad5-CMV-NIS or the tumor-specific Ad5-AFP-NIS systemically via tail vein injection.

Radionuclide uptake studies in vivo

Four days after intratumoral or intravenous injection of Ad5-AFP-NIS, Ad5-control, or Ad5-CMV-NIS, mice received 18.5 MBq (0.5 mCi) of ^{123}I or 111 MBq (3 mCi) of ^{188}Re intraperitoneally and radionuclide biodistribution was monitored by serial imaging on a γ -camera (Forte; ADAC Laboratories/Philips, Milpitas, CA) equipped with a VXHR (Vantage extra high-resolution) collimator (^{123}I) or a medium-energy general purpose (MEGP) collimator (^{188}Re) as described previously (Willhauck *et al.*, 2007, 2008a). Regions of interest were quantified and expressed as a fraction of the total amount of applied radionuclide per gram of tumor tissue. The retention time within the tumor was determined by serial scanning after radionuclide injection and dosimetric calculations were performed according to the concept of medical internal radiation dose (MIRD), with the dose factor of the RADAR (Radiation Dose Assessment Resource) group (www.doseinfo-radar.com).

Analysis of NIS mRNA expression, using quantitative real-time PCR

After infection with Ad5-AFP-NIS total RNA was isolated from HepG2 xenografts, using a RNeasy mini kit (Qiagen, Hilden, Germany) according to the manufacturer's recommendations. Single-stranded oligo(dT)-primer cDNA was generated with SuperScript III reverse transcriptase (Invitrogen Life Technologies). The following primers were used: human NIS (5'-TGCGGGACTTTGAGTACATT-3' and 5'-TG CAGATAATCCGGTGGACA-3') and glyceraldehyde-3-

phosphate dehydrogenase (GAPDH; 5'-GAGAAGGCTG GGGCTCATTT-3' and 5'-CAGTGGGGACACGGAAGG-3'). Quantitative real-time PCR (qPCR) was performed with the cDNA from 1 μ g of RNA, using SYBR green PCR master mix (Qiagen) in a Rotor-Gene 6000 (Corbett Research/Qiagen, Mortlake, New South Wales, Australia). Relative expression levels were calculated by the comparative $\Delta\Delta C_t$ method, using internal GAPDH for normalization.

Indirect immunofluorescence assay

Indirect immunofluorescence staining with an antibody against Ki67 (Abcam, Cambridge, UK) was performed on frozen tissue sections as described previously (Willhauck *et al.*, 2007).

Immunohistochemical analysis of NIS protein expression

Immunohistochemical staining of frozen tissue sections derived from HepG2 xenografts after adenovirus-mediated gene delivery was performed as described previously (Spitzweg *et al.*, 2007). For histological examination parallel slides were also routinely stained with hematoxylin and eosin.

Western blot analysis

Membrane proteins were prepared from virus-infected HepG2 xenografts as described previously (Castro *et al.*, 1999) and subjected to electrophoresis on a 4–12% Bis-Tris HCl-buffered polyacrylamide gel. After transfer of proteins to nitrocellulose membranes by electroblotting, membranes were preincubated in 2% low-fat dried milk in TBS-T (20 mM Tris, 137 mM NaCl, and 0.1% Tween 20). Western blot analysis was performed with a mouse monoclonal antibody directed against amino acid residues 468–643 of human NIS (diluted 1:3000; kindly provided by J.C. Morris, Mayo Clinic, Rochester, MN) as described previously (Spitzweg *et al.*, 1999).

Radionuclide therapy study in vivo

Four days after local virus application (3×10^9 PFU), four groups of mice (^{131}I group, Ad5-AFP-NIS [$n=6$]; ^{188}Re group, Ad5-AFP-NIS [$n=6$]; and control groups with Ad5-control and ^{131}I [$n=6$] or ^{188}Re [$n=6$]) were administered 55.5 MBq (1.5 mCi) of ^{131}I or ^{188}Re per mouse by a single intraperitoneal injection, whereas two other control groups (saline groups, Ad5-AFP-NIS [$n=6$] or Ad5-control [$n=6$]) were treated with saline instead of radionuclides. Tumor size was measured before and twice per week after treatment for up to 7 weeks, using a caliper. Tumor volume was estimated according to the following equation: tumor volume = length \times width \times height \times 0.52. Mice were killed before the end of the 7-week observation period, when tumors started to necrotize, exceed a tumor volume of 1500 mm³, or in case of weight loss of more than 10%, or impairment of breathing as well as drinking and eating behavior.

Statistical methods

All *in vitro* experiments were carried out in triplicate. Results are represented as means \pm SD of triplicates. Statistical

analysis of iodide uptake and real-time qPCR experiments were calculated by Wilcoxon rank-sum test whereas the results of the clonogenic assay were analyzed by quasi-Poisson regression analysis.

The statistical significance of *in vivo* experiments was determined by a linear mixed-model approach, regarding mouse-specific random intercepts. Calculations were performed with the lmer function of the lme4 package (version 0.999375-37; Bates and Maechler, 2010) and the coxph function of the survival package (version 2.36-1; Therneau and Lumley, 2009), using R 2.12-0 software. The dependent variable tumor sizes were log-transformed to hold the assumption of a conditional gaussian distribution. Week, substance (dummy coded), group (dummy coded), and the interaction between substance and group (consequently dummy coded) were included as fixed effects. Assumptions of mixed linear regression could be verified.

Survival data were analyzed using hazard rates modeling the risk of reaching the end point "death" in the next moment. We have assumed the hazard rates to be proportional. Estimation of the virus type effects on the hazard rate was computed using a proportional Cox-model fit, regarding covariates substance, group, and the interaction between substance and group.

Results

Iodide uptake studies in vitro

Maximal iodide uptake activity in HepG2 cells was observed 4 days after infection with Ad5-AFP-NIS, when cells showed a 102-fold increase in perchlorate-sensitive ^{125}I accumulation as compared with cells infected with the control virus (Ad5-control) (Fig. 1A; $p < 0.005$). Tumor specificity of Ad5-AFP-NIS was confirmed by infection of control cancer cell lines (LNCaP, 1205Lu) not expressing AFP showing lack of perchlorate-sensitive iodide uptake activity (Fig. 1A).

In vitro clonogenic assay using ^{131}I

An *in vitro* clonogenic assay was performed to determine the therapeutic efficacy of increasing doses of ^{131}I in HepG2 cells after adenovirus-mediated NIS gene transfer (Fig. 1B). Whereas up to 95% of NIS-transduced HepG2 cells were killed in a dose-dependent manner by exposure to ^{131}I ($p < 0.001$), 98% of uninfected HepG2 cells survived the treatment with 29.6 MBq of ^{131}I . Because HepG2 cells infected with Ad5-AFP-NIS without radioiodine treatment (saline only) had similar survival rates, we conclude that virus infection per se had no influence on cell survival of HepG2 cells in this experimental setup (Fig. 1B).

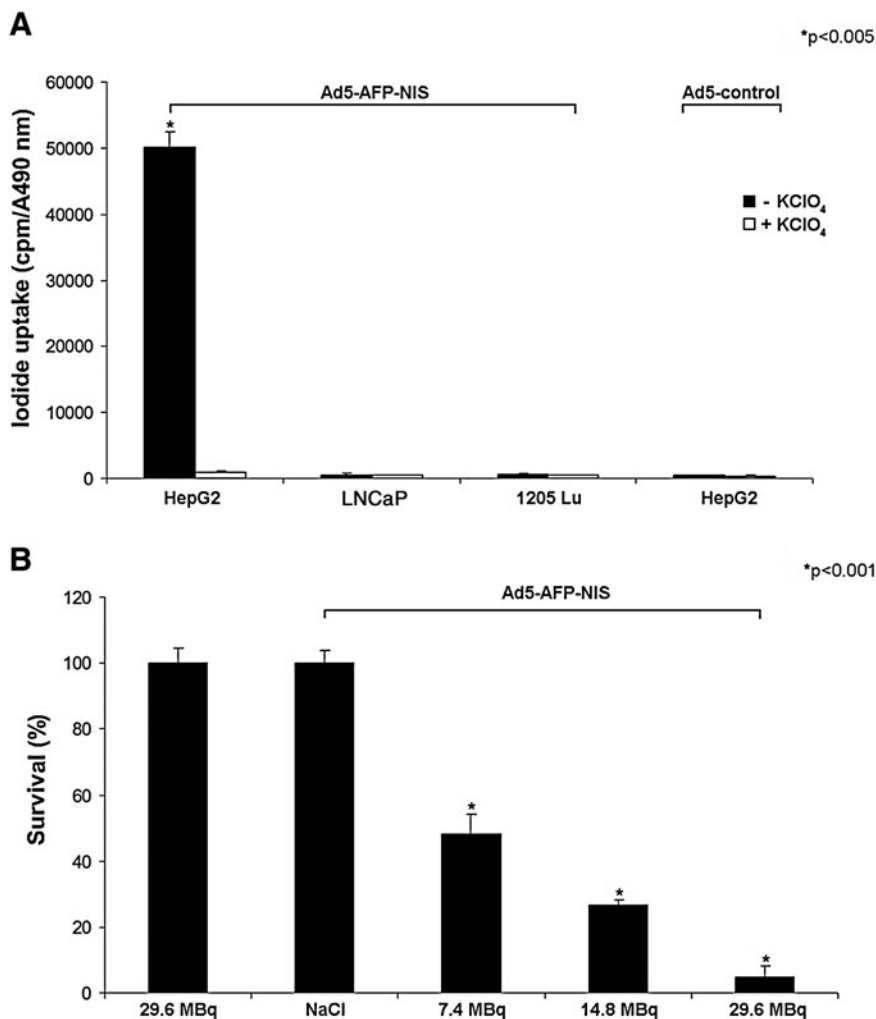


FIG. 1. (A) HepG2 cells infected with Ad5-AFP-NIS showed a 102-fold increase in perchlorate-sensitive ^{125}I accumulation. In contrast, no iodide uptake above background level was observed in HepG2 cells transfected with an Ad5-control virus or in control cells (LNCaP and 1205Lu) transfected with Ad5-AFP-NIS ($*p < 0.005$). (B) In an *in vitro* clonogenic assay, HepG2 cells infected with Ad5-AFP-NIS were exposed to 7.4, 14.8, or 29.6 MBq of ^{131}I , resulting in cell-killing rates of approximately 52, 73, and 95%. Ad5-AFP-NIS-infected HepG2 cells incubated with NaCl, as well as non-infected HepG2 cells incubated with 29.6 MBq of ^{131}I , showed almost no unselective cell death ($*p < 0.001$). Results are expressed as means and SD.

Radionuclide uptake studies after *in vivo* NIS gene transfer

Whereas no radionuclide accumulation was detected in tumors after infection with Ad5-control (left flank), NIS-transduced HepG2 tumors (right flank) showed a significant uptake of ^{123}I and ^{188}Re (Fig. 2A and B). As determined by serial scanning, 14.5% ID/g (percentage of the injected dose per gram of tumor tissue) ^{123}I and 9.2% ID/g ^{188}Re were accumulated 2 hr postinjection in NIS-transduced xenograft tumors with effective half-lives of 13 hr for ^{131}I and 12.8 hr for ^{188}Re . The absorbed doses to the tumor were calculated to be 318 mGy/MBq ^{131}I as compared with 545 mGy/MBq for ^{188}Re . Besides tumoral iodide uptake, significant radioiodine accumulation was observed in tissues physiologically expressing NIS, including stomach and thyroid, as well as in the urinary bladder.

In addition, tumor specificity of Ad5-AFP-NIS was confirmed by infection of control tumor xenografts (LNCaP, 1205Lu), which did not result in tumoral iodide uptake activity (Fig. 2C and D).

Four days after systemic injection of Ad5-CMV-NIS high levels of iodide uptake were observed in the liver because of hepatic pooling of the adenovirus, whereas no iodide accumulation was observed in the tumor (Fig. 3B). In contrast, after administration of Ad5-AFP-NIS we did not observe iodide uptake in nontarget organs, such as liver or lungs, as determined by ^{123}I scintigraphy, whereas a low level of iodide uptake could be detected in HCC xenografts, underlining the tumor specificity and high activity of the AFP promoter used in our study (Fig. 3A). These data were confirmed by *ex vivo* biodistribution analysis by γ -counter analysis showing that 48% ID/g was accumulated in the liver after intravenous injection of Ad5-CMV-NIS, whereas after injection of Ad5-AFP-NIS only 1% ID/g was accumulated in the liver (Fig. 3C) and 3.7% ID/g in the tumor.

Analysis of NIS mRNA expression in HepG2 xenografts

Assessment of NIS mRNA expression after local adenoviral NIS gene transfer *in vivo*, using qPCR analysis, revealed a 33-fold increase in NIS mRNA expression in HepG2 xenografts 4 days after intratumoral injection of Ad5-AFP-NIS as compared with mock-transduced tumors (data not shown).

Western blot analysis

Four days after intratumoral injection of Ad5-AFP-NIS or Ad5-control, NIS protein expression levels were determined in HepG2 cell xenografts by Western blot analysis, revealing a NIS-specific band with a molecular mass of approximately 90 kDa in Ad5-AFP-NIS-infected xenografts, which was not detected in tumors transduced with Ad5-control (Fig. 4A).

Indirect immunofluorescence assay

Indirect immunofluorescence staining revealed 70% Ki67-positive tumor cells in HepG2 xenografts as compared with 35% in LNCaP tumors (data not shown).

Immunohistochemical analysis of NIS protein expression in HepG2 xenografts

Immunohistochemical analysis of HepG2 xenografts revealed a heterogeneous staining pattern with areas of primarily membrane-associated NIS-specific immunoreactivity in tumors after intratumoral application of Ad5-AFP-NIS (Fig. 4B, arrows). In contrast, tumors treated with Ad5-control showed no NIS-specific immunoreactivity (Fig. 4C). Parallel control slides with the primary and secondary antibodies replaced in turn by PBS and isotype-matched

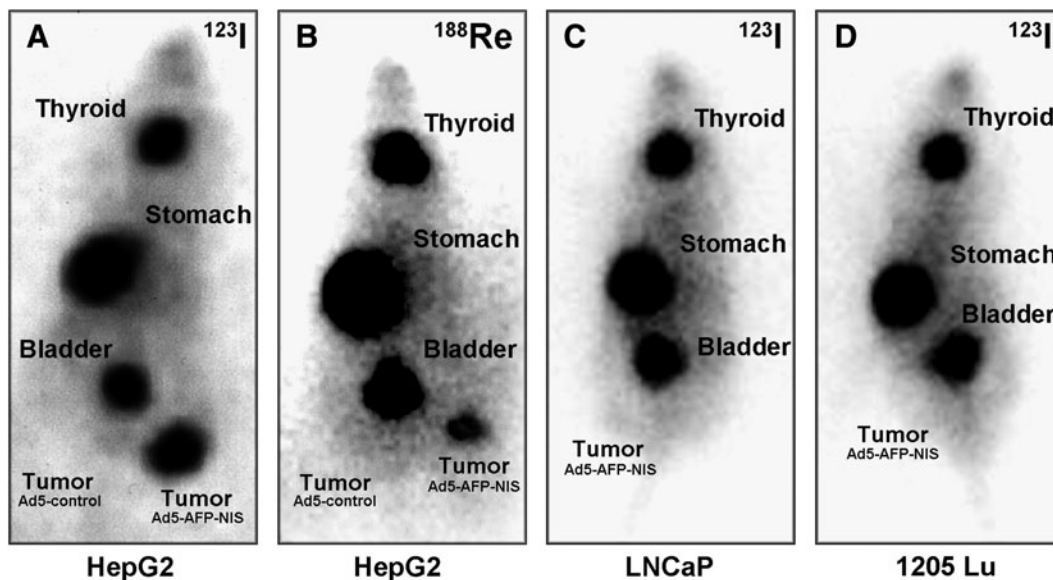


FIG. 2. Radionuclide uptake studies *in vivo*. (A) ^{123}I and (B) ^{188}Re scans of nude mice bearing HepG2 xenografts located on the right and left flanks, 6 hr after administration of ^{123}I or ^{188}Re . Four days after intratumoral injection of Ad5-AFP-NIS (right) and Ad5-control (left) Ad5-AFP-NIS-infected tumors trapped (A) 14.5% ID/g ^{123}I and (B) 9.2% ID/g ^{188}Re , whereas Ad5-control-infected tumors showed no radionuclide uptake (A and B). In contrast, control (C) LNCaP xenografts and (D) 1205Lu xenografts infected with Ad5-AFP-NIS showed no tumoral iodide accumulation.

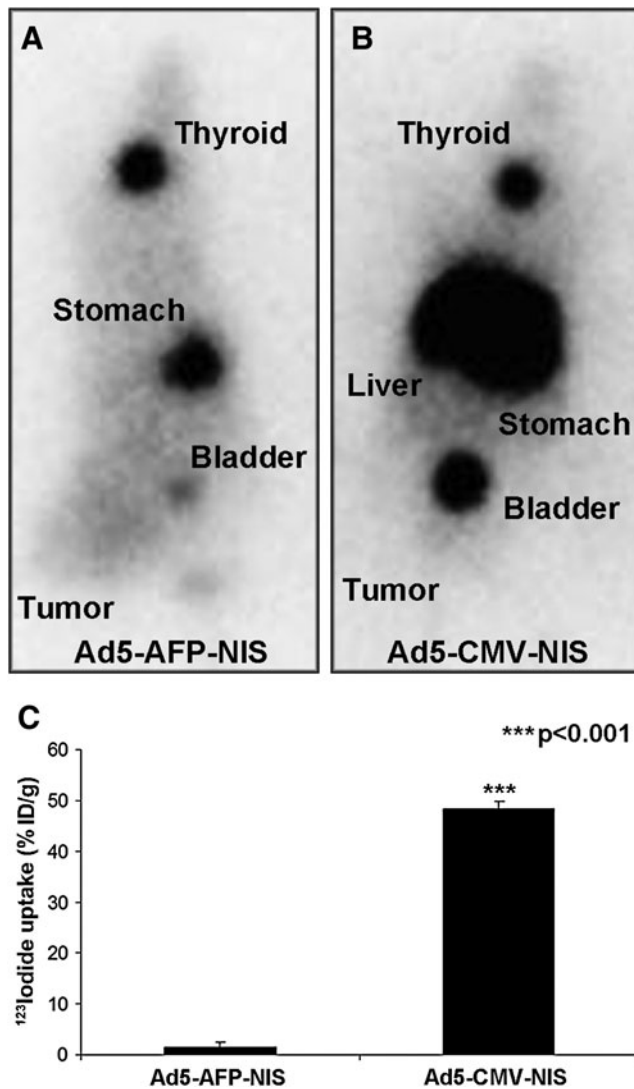


FIG. 3. *In vivo* imaging of ^{123}I biodistribution in nude mice 4 days after intravenous administration of (A) Ad5-AFP-NIS or (B) Ad5-CMV-NIS. After application of Ad5-CMV-NIS high levels of iodide accumulation were observed in the liver without iodide uptake in the tumor (B). In contrast, after application of Ad5-AFP-NIS no iodide accumulation was observed in the liver or other nontarget organs, whereas a low level of iodide uptake was observed in the tumor (3.7% ID/g) (A). (C) γ -Counter analysis showed accumulation of 48% ID/g in the liver after injection of Ad5-CMV-NIS, whereas livers of Ad5-AFP-NIS-injected mice accumulated only 1% ID/g. Results are expressed as means and SD ($***p < 0.001$).

nonimmune immunoglobulin were negative (data not shown).

Radionuclide therapy study *in vivo*

All saline-treated tumors and tumors infected with the control virus continued their growth throughout the observation period (increase in tumor size: Ad5-control/ ^{131}I , 26.9-fold; Ad5-control/ ^{188}Re , 25.2-fold; Ad5-control/saline, 24.5-fold; Ad5-AFP-NIS/saline, 23-fold) (Fig. 5A). In contrast, NIS-transduced tumors showed a significant delay in tumor growth

after injection of ^{131}I or ^{188}Re ($p < 0.005$). Three to 5 weeks after radionuclide injection the therapeutic efficacy of ^{188}Re seemed to be more pronounced as compared with ^{131}I , but differences were mild without reaching statistical significance. Whereas all of the mice in the control groups had to be killed within the first 5 weeks after onset of the experiments, due to excessive tumor growth, 85% of mice treated with ^{131}I or ^{188}Re after local *in vivo* NIS gene transfer survived approximately 7–8 weeks (Fig. 5B). None of the mice showed major adverse effects after virus or radionuclide administration in terms of body weight loss, lethargy or respiratory failure.

Histological evaluation of HepG2 xenografts showed a significant degree of necrosis in NIS-transduced tumors 4 weeks after radionuclide treatment (^{131}I or ^{188}Re), whereas saline-treated tumors exhibited only small areas of necrosis (data not shown).

Discussion

In its dual role as reporter and therapy gene, NIS allows direct, noninvasive imaging of functional NIS expression by ^{123}I scintigraphy and ^{124}I positron emission tomographic imaging as well as exact dosimetric calculations before proceeding to therapeutic application of ^{131}I or alternative radionuclides (Spitzweg and Morris, 2002; Dingli *et al.*, 2003b; Hingorani *et al.*, 2010). Our initial work in the prostate cancer model followed by several studies in a variety of tumor models have clearly demonstrated the enormous potential of NIS as one of the oldest and most successful targets of molecular imaging and radionuclide (^{131}I , ^{188}Re , ^{211}At) therapy (Spitzweg *et al.*, 1999, 2000, 2007; Kakinuma *et al.*, 2003; Cengic *et al.*, 2005; Dwyer *et al.*, 2006a; Scholz *et al.*, 2005; Willhauck *et al.*, 2007, 2008a).

In liver cancer Chen and colleagues reported that a halting of tumor growth could be achieved *in vivo* in a subcutaneous HCC rat model after ^{131}I application after retroviral NIS gene transfer under the control of the albumin promoter (Chen *et al.*, 2006). However, application of the albumin promoter implies the problem of possible substantial toxicity to normal hepatocytes. We have therefore chosen to apply the tumor-specific AFP promoter to transcriptionally target NIS expression selectively to liver cancer cells, thereby minimizing toxicity in normal liver cells and other organs (Willhauck *et al.*, 2008b).

As a next step toward clinical application of the NIS gene therapy approach in patients with liver cancer, in the current study we performed *in vivo* NIS gene transfer into HCC xenograft tumors using a replication-deficient human adenovirus carrying the human NIS gene linked to the tumor-specific AFP promoter (Ad5-AFP-NIS). After *in vitro* characterization of Ad5-AFP-NIS in human HCC cells, HepG2 tumors injected with Ad5-AFP-NIS were demonstrated to accumulate 14.5% and 9.2% ID/g of the total administered ^{123}I and ^{188}Re , respectively, due to tumor-specific NIS expression as confirmed by real-time qPCR and Western blot analysis. These data are consistent with previous biodistribution studies in various tumor models showing higher amounts of accumulated iodide than ^{188}Re in NIS-expressing tumors, suggesting a higher affinity of NIS for iodide than for ^{188}Re (Kang *et al.*, 2004; Dadachova *et al.*, 2005; Willhauck *et al.*, 2007). In our study, a tumor-absorbed dose of 545 mGy/MBq ^{188}Re was calculated, which was 1.7 times higher than

FIG. 4. (A) Western blot analysis revealed a major NIS-specific band of approximately 90 kDa in Ad5-AFP-NIS-infected HepG2 xenografts, whereas Ad5-control-infected HepG2 xenografts did not show NIS protein expression. **(B)** Immunohistochemical staining of HepG2 xenografts after infection with Ad5-AFP-NIS showed heterogeneous, primarily membrane-associated NIS-specific immunoreactivity. **(C)** In contrast, HepG2 xenografts infected with Ad5-control did not reveal NIS-specific immunoreactivity. Original magnification: $\times 400$. Color images available online at www.liebertonline.com/hum

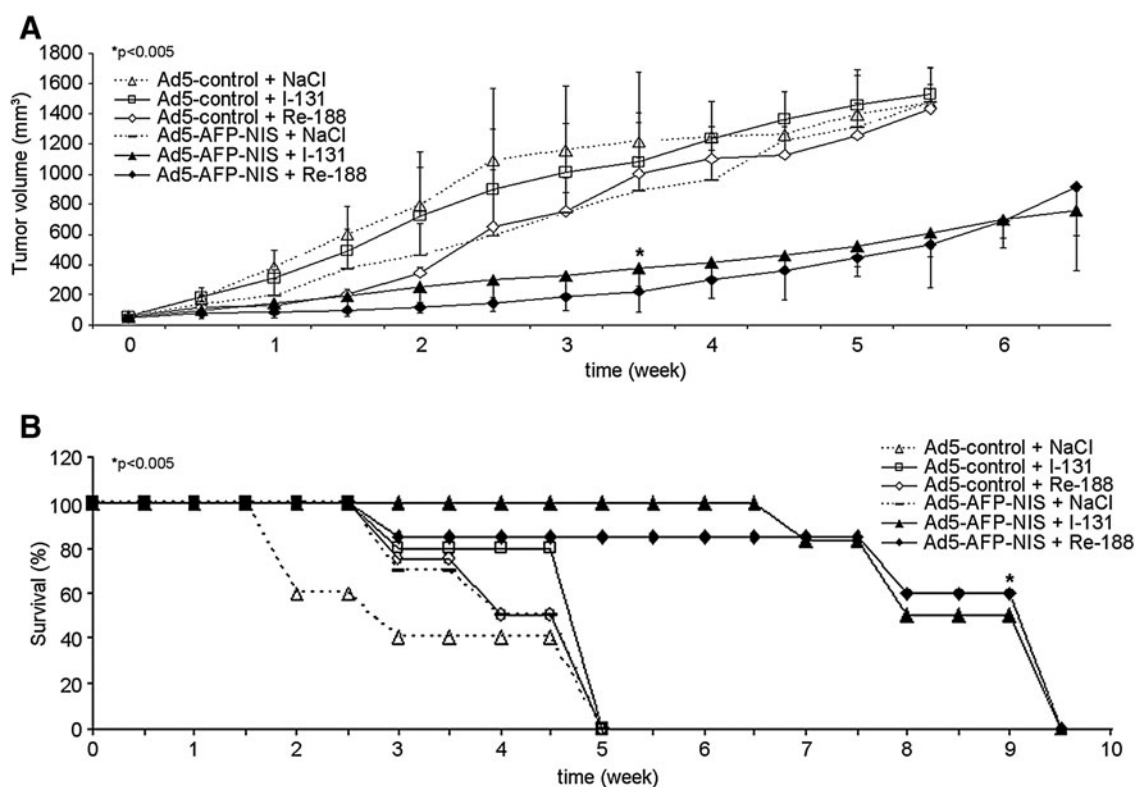
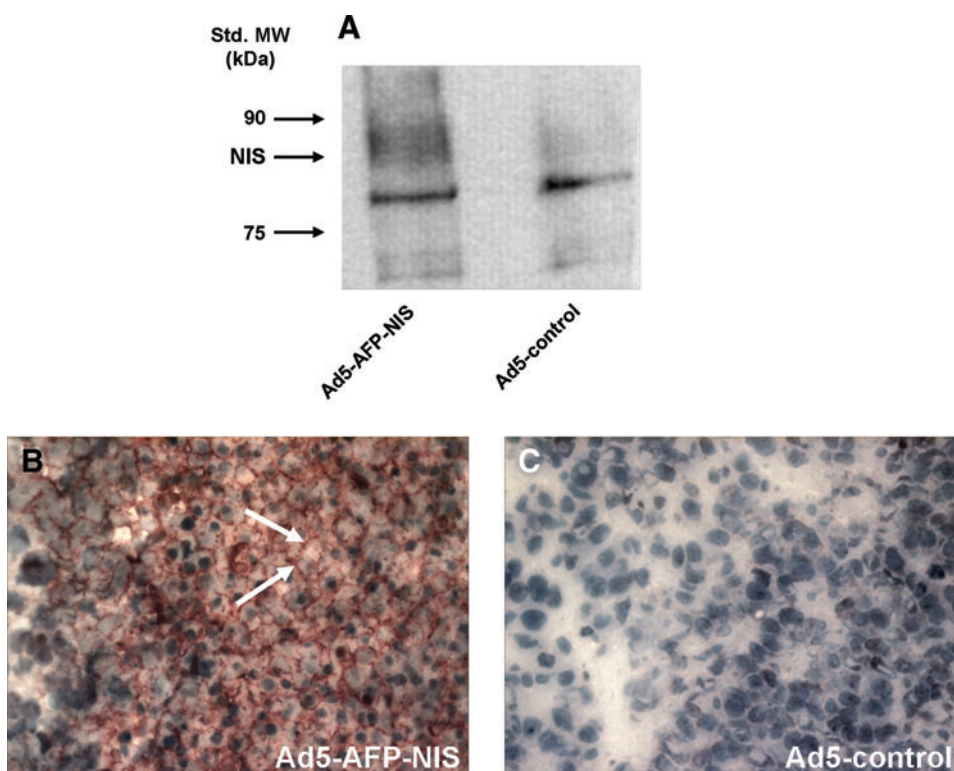


FIG. 5. Radionuclide therapy studies *in vivo*. Growth of Ad5-AFP-NIS-infected HepG2 xenografts (solid symbols) and Ad5-control-infected HepG2 xenografts (open symbols) in nude mice after injection of ¹³¹I, ¹⁸⁸Re (solid lines), or saline (dashed lines). Radionuclide therapy after intratumoral injection of Ad5-AFP-NIS resulted in a significant delay of tumor growth (A, $*p < 0.005$) that was associated with markedly improved survival (B, Kaplan-Meier plot) as compared with control groups ($*p < 0.005$).

for ^{131}I (318 mGy/MBq). In contrast, Dadachova and colleagues showed a radiation dose 4.5 times higher for ^{188}Re than for ^{131}I in NIS-expressing mammary adenocarcinomas in MMTV-NeuT mice (Dadachova *et al.*, 2005). Similarly, in one of our earlier studies in NIS-expressing prostate cancer xenografts, the tumor-absorbed dose was increased 4.5-fold after application of ^{188}Re as compared with ^{131}I (Willhauck *et al.*, 2007). This difference might be due to the more inhomogeneous NIS expression pattern as shown by immunohistochemical staining and therefore heterogeneous radionuclide accumulation after adenoviral *in vivo* NIS gene transfer as compared with stably or endogenously NIS-expressing tumor models in the former studies.

To further confirm tumor specificity of the AFP promoter construct we administered Ad5-AFP-NIS systemically via the tail vein, which did not result in any iodide uptake in the liver or other nontarget organs, demonstrating the selectivity and safety of this construct, despite the significant adenovirus pooling in the liver as demonstrated by intravenous application of the unspecific Ad5-CMV-NIS. Interestingly, even after systemic tail vein injection of Ad5-AFP-NIS, enough viral particles reached the peripheral HCC xenografts to induce a low level of iodide uptake of approximately 4% ID/g, demonstrating the high tumor specificity and promoter activity of our adenoviral vector. These data confirm that transcriptional tumor targeting by application of the AFP promoter allows the restriction of NIS expression to tumor cells to avoid toxicity to normal hepatocytes, suggesting a safe gene transfer method even in the case of virus leakage or after systemic application.

Besides tumoral iodide uptake, significant radioiodine accumulation was observed in tissues physiologically expressing NIS, including the stomach and thyroid gland, as well as in the urinary bladder, due to elimination of radioiodine through the kidneys. In this context it is important to mention that because of the exquisite regulation of thyroidal NIS expression by thyroid-stimulating hormone (TSH), ^{123}I accumulation in the thyroid gland can effectively be down-regulated by thyroid hormone treatment as shown in humans (Wapnir *et al.*, 2004). Further, uptake in the stomach appears to be higher than is usually seen in humans, which is most probably caused by pooling of gastric juices due to the anesthesia for a prolonged period during the imaging procedure. In addition, by stimulation of diuresis the radioiodine retention time in the bladder can be effectively shortened, thereby minimizing the delivered dose and avoiding side effects to the bladder and adjacent tissues.

Our comparative ^{131}I and ^{188}Re therapy experiments after intratumoral *in vivo* NIS gene transfer in HepG2 xenografts showed significantly delayed tumor growth, which was associated with markedly improved survival. However, the therapeutic effect of the NIS-mediated radionuclide therapy was less prominent in the current study as compared with earlier studies in other tumor models showing tumor volume reductions of up to 80–90% (Spitzweg *et al.*, 2000, 2001a; Dingli *et al.*, 2003a; Faivre *et al.*, 2004; Dwyer *et al.*, 2006b; Willhauck *et al.*, 2007, 2008b), which is probably due to the extraordinarily high proliferation rate of HepG2 tumors that showed a Ki67 index of approximately 70% in contrast to 35% in the LNCaP tumors used in our earlier studies (Spitzweg *et al.*, 2000, 2001a; Willhauck *et al.*, 2007, 2008a). Further, histological examination of treated HepG2 tumors

revealed a significant degree of necrosis after radionuclide therapy with ^{131}I or ^{188}Re , which was not seen after application of saline, suggesting significant therapeutic efficacy. These data also demonstrate that measurement of tumor size alone is not sufficient for proper analysis of the therapeutic efficacy of molecularly targeted therapies including NIS-mediated radionuclide therapy. It will therefore be important to analyze antiproliferative and antiangiogenic effects by *ex vivo* immunohistochemical analysis as well as *in vivo* imaging modalities, which are currently being studied.

Our data are consistent with previously published studies showing significant therapeutic efficacy of NIS-mediated radioiodide therapy in HCC. Faivre and colleagues, who applied an adenovirus carrying the rat NIS gene under the control of the CMV promoter intratumorally or via the portal vein, demonstrated strong tumor growth inhibition up to complete tumor regression after application of ^{131}I in an HCC rat model (Faivre *et al.*, 2004). In a more recent study, Herve and colleagues applied a recombinant adenovirus carrying the NIS gene under the control of the tumor-specific hepatocarcinoma-intestine-pancreas promoter intratumorally or via the hepatic artery, showing growth inhibition of orthotopic liver tumors after application of ^{131}I (Herve *et al.*, 2008).

In contrast to our earlier study in the prostate cancer model (Willhauck *et al.*, 2007), application of ^{188}Re did not result in a significant increase in therapeutic efficacy in HepG2 xenografts after adenoviral NIS gene transfer as compared with ^{131}I , which is consistent with the dosimetry data as outlined previously. An additional reason could be the smaller tumor sizes we had to use in the current model, due to the aggressive growth behavior of HepG2 cells, attenuating the stimulation of the crossfire effect, which can be expected after application of ^{188}Re on the basis of its longer path length of up to 10.4 mm as compared with ^{131}I (2.4 mm).

In conclusion, a therapeutic effect of ^{131}I and ^{188}Re has been demonstrated in HCC xenografts after transcriptionally targeted intratumoral *in vivo* NIS gene transfer, showing the proof of principle of AFP promoter-controlled and NIS-mediated radionuclide therapy in liver cancer. Because the ultimate goal of this project is to establish a novel therapeutic approach for metastatic HCC, we have begun to develop replication-competent adenoviral vectors that are designed to replicate under the control of the AFP promoter in order to enhance tumor-specific transduction efficacy after systemic application as well as therapeutic effect by an additional oncolytic effect. Provided that further studies aiming at systemic and regional *in vivo* gene delivery in orthotopic multifocal HCC models will confirm the therapeutic efficacy of AFP promoter-targeted NIS gene therapy, these data clearly demonstrate the potential of NIS as a novel therapeutic gene allowing targeted radionuclide therapy of HCC.

Acknowledgments

The authors are grateful to S.M. Jhiang (Ohio State University, Columbus, OH) for supplying the full-length human NIS cDNA, to M. Geissler (Esslingen, Germany) for supplying the murine AFP promoter/enhancer fragment, and to J. C. Morris (Mayo Clinic, Rochester, MN) for providing the NIS mouse monoclonal antibody. The authors also thank R.

Anderson (ViraQuest, North Liberty, IA) for the synthesis of Ad5-AFP-NIS, as well as H. Reulen (Munich, Germany) for expert statistical calculations. This study was supported by Grant SFB 824 (Sonderforschungsbereich 824) from the Deutsche Forschungsgemeinschaft (Bonn, Germany) and by a grant from the Wilhelm-Sander-Stiftung (2008.037.1) to C. Spitzweg.

Author Disclosure Statement

No competing financial interest exists.

References

- Bates, D., and Maechler, M. (2010). *lme4: Linear mixed-effects models using S4 classes*. R package version 0.999375-37. Available at <http://CRAN.R-project.org/package=lme4> (accessed June 2011).
- Castro, M.R., Bergert, E.R., Beito, T.G., et al. (1999). Monoclonal antibodies against the human sodium iodide symporter: Utility for immunocytochemistry of thyroid cancer. *J. Endocrinol.* 163, 495–504.
- Cengic, N., Baker, C.H., Schutz, M., et al. (2005). A novel therapeutic strategy for medullary thyroid cancer based on radioiodine therapy following tissue-specific sodium iodide symporter gene expression. *J. Clin. Endocrinol. Metab.* 90, 4457–4464.
- Chen, L., Altmann, A., Mier, W., et al. (2006). Radioiodine therapy of hepatoma using targeted transfer of the human sodium iodide symporter gene. *J. Nucl. Med.* 47, 854–862.
- Dadachova, E., Nguyen, A., Lin, E.Y., et al. (2005). Treatment with rhenium-188-perrhenate and iodine-131 of NIS-expressing mammary cancer in a mouse model remarkably inhibited tumor growth. *Nucl. Med. Biol.* 32, 695–700.
- Dai, G., Levy, O., and Carrasco, N. (1996). Cloning and characterization of the thyroid iodide transporter. *Nature* 379, 458–460.
- Dingli, D., Diaz, R.M., Bergert, E.R., et al. (2003a). Genetically targeted radiotherapy for multiple myeloma. *Blood* 102, 489–496.
- Dingli, D., Russell, S.J., and Morris, J.C., III. (2003b). *In vivo* imaging and tumor therapy with the sodium iodide symporter. *J. Cell Biochem.* 90, 1079–1086.
- Dingli, D., Peng, K.-W., Harvey, M.E., et al. (2004). Image-guided radiotherapy for multiple myeloma using a recombinant measles virus expressing the thyroidal sodium iodide symporter. *Blood* 103, 1641–1646.
- Dwyer, R.M., Bergert, E.R., O'Connor, M.K., et al. (2005a). *In vivo* radioiodide imaging and treatment of breast cancer xenografts after MUC1-driven expression of the sodium iodide symporter. *Cancer Res.* 11, 1483–1489.
- Dwyer, R.M., Bergert, E.R., O'Connor, M.K., et al. (2006a). Sodium iodide symporter-mediated radioiodide imaging and therapy of ovarian tumor xenografts in mice. *Gene Ther.* 13, 60–66.
- Dwyer, R.M., Bergert, E.R., O'Connor, M.K., et al. (2006b). Adenovirus-mediated and targeted expression of the sodium iodide symporter permits *in vivo* radioiodide imaging and therapy of pancreatic tumors. *Hum. Gene Ther.* 17, 661–668.
- Faivre, J., Clerc, J., Gerolami, R., et al. (2004). Long-term radioiodine retention and regression of liver cancer after sodium iodide symporter gene transfer in Wistar rats. *Cancer Res.* 64, 8045–8051.
- Hart, I.R. (1996). Tissue specific promoters in targeting systemically delivered gene therapy. *Semin. Oncol.* 23, 154–158.
- Herve, J., Cunha, A.S., Liu, B., et al. (2008). Internal radiotherapy of liver cancer with rat hepatocarcinoma-intestine-pancreas gene as a liver tumor-specific promoter. *Hum. Gene Ther.* 19, 915–926.
- Hingorani, M., Spitzweg, C., Vassaux, G., et al. (2010). The biology of the sodium iodide symporter and its potential for targeted gene delivery. *Curr. Cancer Drug Targets* 10, 242–267.
- Kakinuma, H., Bergert, E.R., Spitzweg, C., et al. (2003). Probasin promoter (ARR₂PB)-driven, prostate-specific expression of the human sodium iodide symporter (h-NIS) for targeted radioiodine therapy of prostate cancer. *Cancer Res.* 63, 7840–7844.
- Kang, J.H., Chung, J.K., Lee, Y.J., et al. (2004). Establishment of a human hepatocellular carcinoma cell line highly expressing sodium iodide symporter for radionuclide gene therapy. *J. Nucl. Med.* 45, 1571–1576.
- Li, H., Peng, K.W., Dingli, D., et al. (2010). Oncolytic measles viruses encoding interferon β and the thyroidal sodium iodide symporter gene for mesothelioma virotherapy. *Cancer Gene Ther.* 17, 550–558.
- Mandell, R.B., Mandell, L.Z., and Link, C.J., Jr. (1999). Radioisotope concentrator gene therapy using the sodium/iodide symporter gene. *Cancer Res.* 59, 661–668.
- Peerlinck, I., Merron, A., Baril, P., et al. (2009). Targeted radioiodide therapy using a Wnt-targeted replicating adenovirus encoding the Na/I symporter. *Clin. Cancer Res.* 15, 6595–6601.
- Penheiter, A.R., Wegman, T.R., Classic, K.L., et al. (2010). Sodium iodide symporter (NIS)-mediated radiovirotherapy for pancreatic cancer. *AJR Am. J. Roentgenol.* 195, 341–349.
- Scholz, I.V., Cengic, N., Baker, C.H., et al. (2005). Radioiodine therapy of colon cancer following tissue-specific sodium iodide symporter gene transfer. *Gene Ther.* 12, 272–280.
- Smanik, P.A., Liu, Q., Furminger, T.L., et al. (1996). Cloning of the human sodium iodide symporter. *Biochem. Biophys. Res. Commun.* 226, 339–345.
- Spitzweg, C., and Morris, J.C. (2002). The sodium iodide symporter: Its pathophysiological and therapeutic implications. *Clin. Endocrinol.* 57, 559–574.
- Spitzweg, C., Zhang, S., Bergert, E.R., et al. (1999). Prostate-specific antigen (PSA) promoter-driven androgen-inducible expression of sodium iodide symporter in prostate cancer cell lines. *Cancer Res.* 59, 2136–2141.
- Spitzweg, C., O'Connor, M.K., Bergert, E.R., et al. (2000). Treatment of prostate cancer by radioiodine therapy after tissue-specific expression of the sodium iodide symporter. *Cancer Res.* 60, 6526–6530.
- Spitzweg, C., Dietz, A.B., O'Connor, M.K., et al. (2001a). *In vivo* sodium iodide symporter gene therapy of prostate cancer. *Gene Ther.* 8, 1524–1531.
- Spitzweg, C., Harrington, K.J., Pinke, L.A., et al. (2001b). Clinical review 132: The sodium iodide symporter and its potential role in cancer therapy. *J. Clin. Endocrinol. Metab.* 86, 3327–3335.
- Spitzweg, C., Baker, C.H., Bergert, E.R., et al. (2007). Image-guided radioiodide therapy of medullary thyroid cancer after carcinoembryonic antigen promoter-targeted sodium iodide symporter gene expression. *Hum. Gene Ther.* 18, 916–924.
- Therneau, T., and Lumley, T. (2009). *survival: Survival analysis, including penalised likelihood*. R package version 2.35-4. Available at <http://CRAN.R-project.org/package=survival> (accessed June 2011).

- Trujillo, M.A., O'Neal, M.J., McDonough, S., *et al.* (2010) A probasin promoter, conditionally replicating adenovirus that expresses the sodium iodide symporter (NIS) for radiovirotherapy of prostate cancer. *Gene Ther.* 17, 1325–1332.
- Unterholzner, S., Willhauck, M.J., Cengic, N., *et al.* (2006). Dexamethasone stimulation of retinoic acid-induced sodium iodide symporter expression and cytotoxicity of ¹³¹I in breast cancer cells. *J. Clin. Endocrinol. Metab.* 91, 69–78.
- Wapnir, I.L., Goris M, Yudd A, *et al.* (2004). The Na⁺/I⁻ symporter mediates iodide uptake in breast cancer metastases and can be selectively down-regulated in the thyroid. *Clin. Cancer Res* 10, 4294–4302.
- Weiss, S.J., Philp, N.J., and Grollmann E.F. (1984). Iodide transport in a continuous line of cultured cells from rat thyroid. *Endocrinology* 114, 1090–1098.
- Willhauck, M.J., Sharif Samani, B.R., Gildehaus, F.J., *et al.* (2007). Application of ¹⁸⁸rhenium as an alternative radionuclide for treatment of prostate cancer after tumor-specific sodium iodide symporter gene expression. *J. Clin. Endocrinol. Metab.* 92, 4451–4458.
- Willhauck, M.J., Samani, B.R., Wolf, I., *et al.* (2008a). The potential of ²¹¹Astatine for NIS-mediated radionuclide therapy in prostate cancer. *Eur. J. Nucl. Med. Mol. Imaging* 35, 1272–1281.
- Willhauck, M.J., Sharif Samani, B.R., Klutz, K., *et al.* (2008b). α -Fetoprotein promoter-targeted sodium iodide symporter gene therapy of hepatocellular carcinoma. *Gene Ther.* 15, 214–223.

Address correspondence to:

Prof. Dr. Christine Spitzweg
Medizinische Klinik II–Campus Grosshadern
Klinikum der Universität München
Marchioninistrasse 15
81377 Munich
Germany

E-mail: Christine.Spitzweg@med.uni-muenchen.de

Received for publication July 30, 2010;
accepted after revision April 12, 2011.

Published online: April 13, 2011.